Neutron scattering studies on the vibrational excitations and the structure of ordered niobium hydrides: the λ phases

2004 J. Phys.: Condens. Matter 16 5205

(http://iopscience.iop.org/0953-8984/16/29/013)

INSTITUTE OF PHYSICS PUBLISHING JOURNAL OF PHYSICS: CONDENSED MATTER

J. Phys.: Condens. Matter **16** (2004) 5205–5228 PII: S0953-8984(04)73846-1

Neutron scattering studies on the vibrational excitations and the structure of ordered niobium hydrides: the λ phases

B Hauer[1,5], R Hempelmann[2], T J Udovic[3], J J Rush[3], W Kockelmann[4], W Schäfer[4], E Jansen[4] and D Richter[1]

[1] Institut für Festkörperforschung, Forschungszentrum Jülich, D-52425 Jülich, Germany
[2] Physikalische Chemie, Universität des Saarlandes, D-66041 Saarbrücken, Germany
[3] National Institute of Standards and Technology, Gaithersburg, MD 20899, USA
[4] Mineralogisches Institut der Universität Bonn, Außenstelle Jülich, D-52425 Jülich, Germany

Received 23 December 2003
Published 9 July 2004
Online at stacks.iop.org/JPhysCM/16/5205
doi:10.1088/0953-8984/16/29/013

Abstract

Neutron vibrational spectroscopy and neutron diffraction have been used to study the optical hydrogen vibrations in and the structure of ordered niobium hydrides NbH_x and deuterides NbD_x in the concentration range $0.73 < x < 1.0$ and at temperatures between 13 and 250 K. The measurements performed at temperatures above 200 K confirm the established model of the β phase. Neutron diffraction data collected in the regime of the λ phases ($T < 200$ K, $0.73 < x < 1.0$) show that the structure for $x < 0.85$ is made up of microdomains with β phase structure. Neutron vibrational spectra display up to three families of peaks that can be assigned to three different hydrogen sites: an undisturbed tetrahedral site within the microdomains and two strongly disturbed tetrahedral sites within two different kinds of microdomain boundaries. Incommensurately modulated phases probably exist in this concentration range. For hydrogen concentrations around $x \approx 0.85$ there is evidence for a change of symmetry of the basic cell as well as a change of the modulation at even higher concentrations. In the range of the γ phase at $x \approx 0.9$, strong isotopic effects occur. The results give new insights into the phase diagram.

1. Introduction

The niobium hydrogen system can be considered as a prototype system for metal hydrides [1–3]. A long lasting scientific debate concerns the ordered niobium hydrides which were the subject of our neutron scattering studies. In [4] we presented results concerning the ε phase.

[5] Present address: Forschungsinstitut der Zementindustrie, Tannenstrasse 2, D-40476 Düsseldorf, Germany.

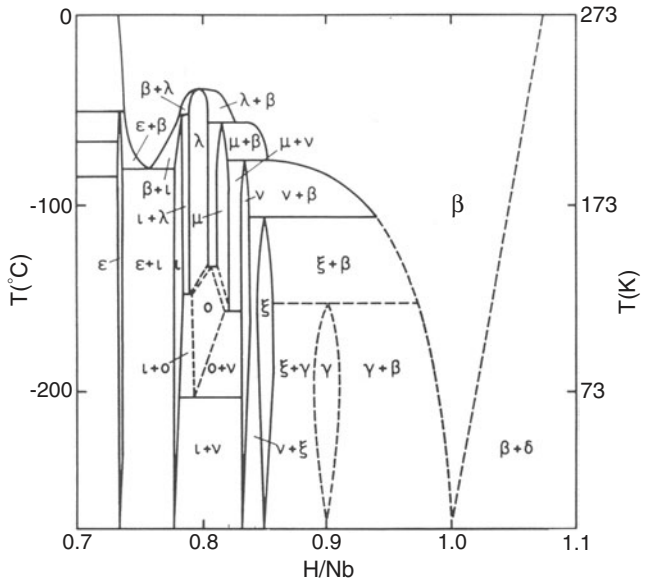

Figure 1. A partial low temperature Nb–H phase diagram depicting the λ phase region [6].

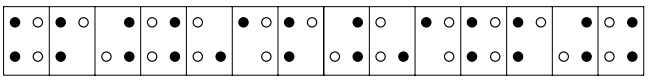

Figure 2. The structure of the λ phases according to [5, 7]. A sequence of two kinds of microdomains with β phase structure in the z direction: ○, H at $\frac{1}{4}[1\bar{1}0]_c$; ●, H at $\frac{3}{4}[1\bar{1}0]_c$.

There we found a splitting of the vibrational levels. This splitting is caused by the coexistence of inequivalent hydrogen sites which differ in their hydrogen potentials due to different distortions of the tetrahedral niobium surroundings. Now we present neutron scattering studies on niobium hydrides and deuterides $NbH(D)_x$ with hydrogen concentrations $0.73 < x < 1.0$ at temperatures $T \leqslant 250$ K. This includes the β phase and several ordered phases. A phase diagram of this region was proposed by Köbler and Welter [6] (figure 1). Seven different phases have been introduced in addition to the ϵ and the β phase which have been denoted as ι, μ, ν, λ, o, ξ, and γ. In many references they are commonly denoted as λ phases or λ phase regions as will be done below. However, neutron scattering [7] and TEM results [5, 8] are at variance with these results of Köbler and Welter. Makenas and Birnbaum [5] also denied the existence of the γ phase proposed by Pick for $x \approx 0.9$ [9]. According to a structure model of the λ phases [5, 7] sequences of two kinds of β phase microdomains alternate along the c direction. These two kinds of cells differ by a rotation of 180° and build up a modulated structure (figure 2). Hydrogen vacancies exist at the microdomain boundaries in order to avoid small hydrogen–hydrogen distances. A correlation exists between the modulation vector $\vec{k}$ and the hydrogen concentration $c_{H,D}$. However, not all questions concerning this structural model have been previously solved, e.g. the structure of the microdomain boundaries and the existence of incommensurate modulated phases. Furthermore, the model is not confirmed yet, although Welter and Schöndube [10] detected superstructure reflections in neutron diffractograms of $NbD_{0.825}$ similar to those measured by Brun *et al* [7]. Hauck had proposed a structure model of the γ phase [11].

Using neutron vibrational spectroscopy, the fundamental hydrogen vibrations have been studied by Eckert *et al* [12], but the energy resolution was not sufficient to resolve the level splittings clearly. Now we have re-investigated the λ phases taking advantage of a high resolution spectrometer. We also performed neutron diffraction measurements in order to examine and refine the proposed structural models of the λ phases.

2. Theory

In metal hydrides, hydrogen atoms can often be approximated as three-dimensional harmonic oscillators. Therefore the vibrational spectrum is determined by the Hamiltonian $\mathcal{H}$:

$$\mathcal{H} = \frac{\vec{p}^2}{2m} + V(x, y, z) \tag{1}$$

with the potential

$$V(x, y, z) = \tfrac{1}{2}m(\omega_x^2 x^2 + \omega_y^2 y^2 + \omega_z^2 z^2) \tag{2}$$

and the energy levels

$$E_{l,m,n} = (l + \tfrac{1}{2})\hbar\omega_x + (m + \tfrac{1}{2})\hbar\omega_y + (n + \tfrac{1}{2})\hbar\omega_z. \tag{3}$$

Only fundamental vibrations are examined in the spectra with $l + m + n = 1$. The theoretical description of neutron scattering is presented in section 4.1.1 below.

The basic structure of the crystal may be modulated by a periodic distortion concerning the position of atoms and the occupation probability of particular sites. In order to handle such modulated structures we have to introduce a modulation vector

$$\vec{k} = (k_x a^* + k_y b^* + k_z c^*) \qquad \text{with } 0 < k_i < 1, \quad i = x, y, z. \tag{4}$$

a^*, b^* and c^* are the basic vectors of the cell in reciprocal space. The modulation is said to be commensurate with the translation symmetry of the basic structure if all components k_i are rational. If one component k_i is irrational, the structure is said to be incommensurately modulated with regard to the cell. In any case, the modulation causes additional satellite peaks in the diffraction patterns. For a modulation in the c direction, only one coefficient k_z has to be taken into account.

3. Experimental details

Neutron vibrational spectroscopy was performed using the beryllium filter spectrometer BT-4 at the research reactor of the National Institute of Standards and Technology (NIST). This spectrometer exhibits two modes: the beryllium filter (bf) mode yielding well resolved spectra with high intensity, and a beryllium graphite filter (bgf) mode yielding spectra with very high resolution but reduced intensity. We used the bf mode in order to investigate the fundamental vibrations in all directions at neutron energy transfers between 100 and 200 meV. The bgf mode was used in order to investigate the fundamental vibrations in the z direction between 100 and 140 meV more thoroughly and to study the hydrogen vibrations of the niobium deuterides.

Most of the samples were prepared using bulk polycrystalline material with a purity of at least 99.9%. The samples of $NbH_{0.920}$ and $NbH_{0.945}$ were prepared using single crystals. The hydrogen loading was performed from the gas phase; the hydrogen content was determined from the weight increase of the samples.

The diffraction data have been collected using the high resolution powder diffractometer BT-1 at NIST which has already been described in [4]. The deuterides investigated, $NbD_{0.788}$, $NbD_{0.852}$ and $NbD_{0.922}$, and the hydride $NbH_{0.794}$ have been powdered and filled into vanadium

cans. Due to the limited volume of the cans only a part of the sample mass used in the neutron vibrational spectroscopic experiments was used.

4. Results

4.1. Neutron vibrational spectroscopy

4.1.1. Data analysis. The contribution of the 'fast neutrons', i.e. the neutron background existing in the reactor hall, was subtracted from the raw data prior to the data evaluation. The differential scattering cross section of the hydrogen atoms is given by

$$\frac{\partial^2\sigma}{\partial\omega\,\partial\Omega} = N_{\mathrm{H}}\frac{k}{k_0}\frac{\sigma_{\mathrm{tot}}}{4\pi}\sum_j z_j f_j S_j(Q,\omega) \tag{5}$$

where N_{H} is the total number of hydrogen atoms, k_0 and k are the initial and final wavenumbers, respectively, and σ_{tot} is the total scattering cross section of the hydrogen isotope. z_j denotes the number of j-type hydrogen sites, f_j the occupation of these sites and S_j the scattering function as a function of the scattering vector $\vec{Q}$ and the neutron energy transfer $\hbar\omega$. This scattering function is given by

$$S(Q,\omega) = \exp(-2W(Q))(\tilde{S}^{\mathrm{a}}(Q,\omega) + \tilde{S}^{\mathrm{o}}(Q,\omega) + \tilde{S}^{\mathrm{oa}}(Q,\omega)) \tag{6}$$

where $\tilde{S}^{\mathrm{a}}$ denotes the contribution of the acoustic (band) phonons (outside our measuring regime), $\tilde{S}^{\mathrm{o}}$ that of the optical phonons and $\tilde{S}^{\mathrm{oa}}$ that of the optoacoustic phonons; $\exp(-2W(Q))$ is the hydrogen Debye–Waller factor. If l, m, n denote the three degrees of freedom connected with the three vibrational directions of the oscillating hydrogen atoms, the contribution $\tilde{S}^{\mathrm{o}}$ is given by

$$\tilde{S}^{\mathrm{o}}(Q,\omega) = \frac{1}{n!}\frac{1}{m!}\frac{1}{l!}\left(\frac{\hbar^2Q^2}{6m_{\mathrm{H}}\omega_1}\right)^n\left(\frac{\hbar^2Q^2}{6m_{\mathrm{H}}\omega_2}\right)^m\left(\frac{\hbar^2Q^2}{6m_{\mathrm{H}}\omega_3}\right)^l \times n(n\omega_1 + m\omega_2 + l\omega_3)\delta(\omega - n\omega_1 - m\omega_2 - l\omega_3). \tag{7}$$

The peaks are described by Gaussian line shapes. Their position is denoted by E; the linewidth σ is the half-width at half-maximum (HWHM). The relative intensity in relation to the largest peak is denoted by I. The optoacoustic contribution $\tilde{S}^{\mathrm{oa}}$ is described by a convolution of $\tilde{S}^{\mathrm{a}}$ and $\tilde{S}^{\mathrm{o}}$. The latter was approximated by an empirical function determined using a measured spectrum of the acoustic (band) modes.

Only fundamental vibrations were measured. According to convention, see e.g. [12, 13], the fundamental mode around 120 meV is attributed to the z direction, whereas the two modes around 160 meV are attributed to the y and to the x direction, respectively. If more than one triplet of fundamental excitations is needed to fit the spectra, these triplets are denoted by I, II and III according to their intensity. All spectra are collected in [14].

4.1.2. Spectra measured at 250 K: the β phase. The bgf spectra have been measured at 250 K for three samples: $NbH_{0.609}$ ($E_z = 116.3(1)$ meV; the spectrum is displayed in [4]), $NbH_{0.794}$ and $NbH_{0.920}$. These spectra can be attributed to the β phase. The excitation energy of the z fundamental peak E_z increases with increasing hydrogen content (see table 1). All fundamental vibrations of the samples $NbH_{0.794}$ (top of figure 7) and $NbH_{0.920}$ have been measured using the bf mode of the spectrometer. The spectra for both samples can be described by a single triplet of peaks with $\omega_x = \omega_y$ and the linewidth $\sigma_x = \sigma_y$. However, the fit of the $NbH_{0.920}$ spectrum is not satisfactory and can be improved by introducing $\omega_x \neq \omega_y$ and $\sigma_x \neq \sigma_y$.

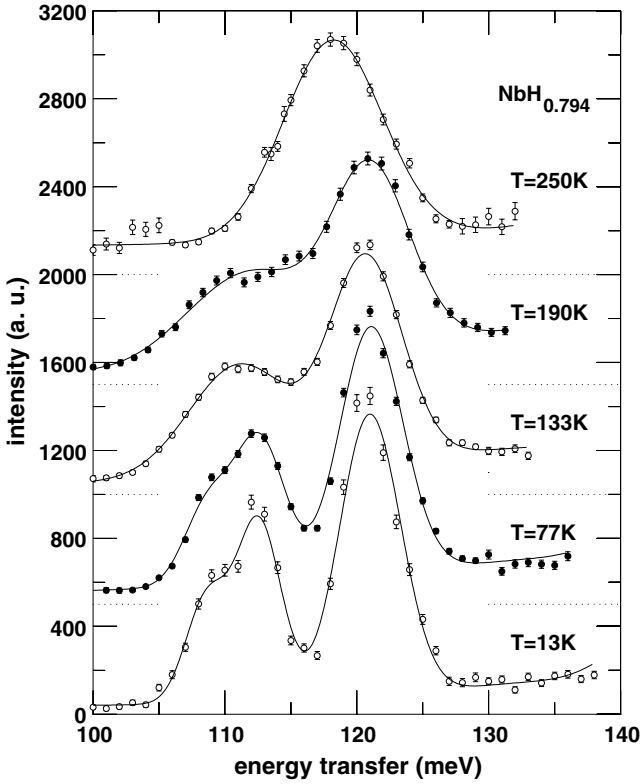

Figure 3. The bgf spectra measured for $NbH_{0.794}$.

4.1.3. Spectra measured below 200 K: λ phases

The bgf spectra measured for the hydrides. In the bgf spectra at hydrogen concentrations $c_H < 0.85$, three peaks can be distinguished at low temperatures. The bgf spectra measured for $NbH_{0.794}$ are shown in figure 3 as an example. We denote the peak at 121 meV by I, the one at 113 meV by II and the peak at 109 meV by III. We coupled $\sigma^{II} = \sigma^{III}$ since the two peaks could not be resolved sufficiently. The intensity ratio of peaks II and III observed at the lowest temperatures was kept fixed at higher temperatures since the peaks broadened and did not allow a clear distinction any longer. Fits with variable parameters, however, yielded no significant improvement.

Fit parameters for all spectra are listed in table 1. The spectra measured for the different concentrations clearly differ in their intensity ratios of the three peaks as discussed below. Nevertheless, the fit parameters describing the peak position and width are very similar even with regard to their temperature dependences.

The bgf spectra of the sample $NbH_{0.920}$ (figure 4) contain only two peaks, i.e., the peak III at 109 meV is missing. The peak II is visible up to 150 K. The temperature dependence of the fit parameters is very similar to those of the spectra described above (see also table 1). Only one peak was detected in the spectra measured for the sample $NbH_{0.945}$.

The bgf spectra measured at 77 K are collected in figure 5. The positions and widths of the observed peaks do not exhibit any significant dependence on the hydrogen concentration of the samples. Only a slight increase in the energy and the width of peak I could be observed. The

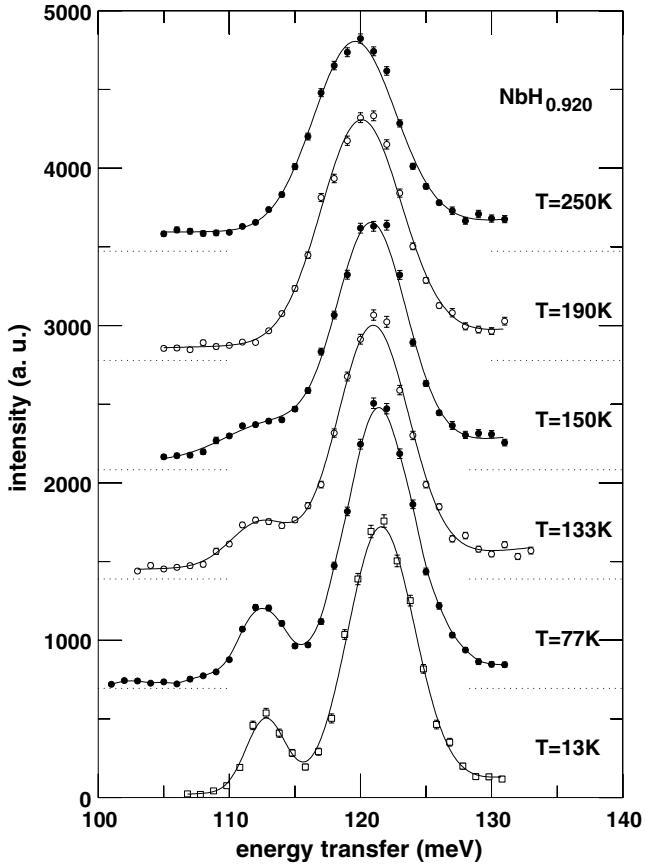

Figure 4. The bgf spectra measured for $NbH_{0.920}$.

relative intensity I of peak III decreases with increasing hydrogen content between $c_H = 0.8$ and 0.85; the intensity of peak II decreases at even higher hydrogen contents above $c_H = 0.85$. The dependence of the relative peak intensities on the hydrogen concentration is shown in figure 6.

The bf spectra of the hydrides. The peaks of the triplets II and III cannot be resolved in the bf mode spectra. Therefore these spectra are fitted assuming two triplets of peaks denoted by I and (II, III). Fit parameters of the triplet (II, III) must be interpreted very cautiously because there may be systematic errors in addition to the statistical errors. The intensity ratio was fitted for the bf spectra obtained at 13 K but not for the spectra measured at higher temperatures. The intensity ratios of the peaks differ from those obtained in the bgf spectra, but the deviation is small.

The bf spectra measured for the samples of $NbH_{0.794}$ are shown in figure 7. The resulting fit parameters are listed in table 2. The fit parameters for $NbH_{0.818}$ and $NbH_{0.843}$ are collected in tables 3 and 4.

The energy of the peaks of triplet I decreases with increasing temperature whereas the widths increase slightly for these three samples. The triplet (II, III) does not show a clear temperature dependence. The spectra obtained at 13 and 77 K are very similar for all samples.

Table 1. The bgf spectra of the excitations in the z direction, observed for niobium hydrides and deuterides with $c_{H,D} > 0.73$. The linewidth σ denotes the half-width at half-maximum (HWHM). The relative *intensities* I are presented in relation to the largest peak ($I = 1.0$).

$NbH_{0.794}$: $I_I = 0.578(19)$, $I_{II} = 0.269(15)$, $I_{III} = 0.153(12)$					
T (K)	E_z^I (meV)	σ_z^I (meV)	E_z^{II} (meV)	$\sigma_z^{II,III}$ (meV)	E_z^{III} (meV)
13	121.0(1)	2.1(1)	112.6(1)	1.1(2)	108.7(2)
77	121.1(1)	2.2(1)	112.7(1)	1.5(2)	108.8(1)
133	120.7(1)	2.8(1)	112.2(4)	3.6(6)	109.0(11)
190	120.2(1)	2.9(1)	112.7(4)	3.8(6)	108.2(7)
250	118.2(1)	4.1(2)			
$NbH_{0.805}$: $I_I = 0.602(23)$, $I_{II} = 0.219(16)$, $I_{III} = 0.179(14)$					
T (K)	E_z^I (meV)	σ_z^I (meV)	E_z^{II} (meV)	$\sigma_z^{II,III}$ (meV)	E_z^{III} (meV)
77	121.3(1)	2.2(1)	112.8(2)	1.6(2)	108.9(2)
$NbH_{0.818}$: $I_I = 0.633(21)$, $I_{II} = 0.231(12)$, $I_{III} = 0.136(10)$					
T (K)	E_z^I (meV)	σ_z^I (meV)	E_z^{II} (meV)	$\sigma_z^{II,III}$ (meV)	E_z^{III} (meV)
13	121.4(2)	2.3(1)	112.6(3)	1.4(2)	108.6(3)
77	121.2(2)	2.3(1)	112.4(3)	1.7(2)	108.4(3)
133	120.7(3)	2.8(1)	112.8(4)	2.9(4)	108.2(6)
190	120.3(3)	3.0(2)	113.0(4)	2.7(3)	108.0(5)
$NbH_{0.835}$: $I_I = 0.677(20)$, $I_{II} = 0.260(14)$, $I_{III} = 0.063(9)$					
T (K)	E_z^I (meV)	σ_z^I (meV)	E_z^{II} (meV)	$\sigma_z^{II,III}$ (meV)	E_z^{III} (meV)
77	121.0(1)	2.2(1)	112.9(1)	1.3(2)	108.7(3)
$NbH_{0.843}$: $I_I = 0.670(24)$, $I_{II} = 0.287(16)$, $I_{III} = 0.043(9)$					
T (K)	E_z^I (meV)	σ_z^I (meV)	E_z^{II} (meV)	$\sigma_z^{II,III}$ (meV)	E_z^{III} (meV)
13	121.1(2)	2.1(1)	113.4(3)	0.8(2)	108.8(5)
77	121.1(1)	2.1(1)	113.2(1)	1.1(1)	108.8(3)
133	120.6(1)	2.3(1)	112.9(1)	2.1(1)	107.5(5)
190	120.3(1)	2.5(1)	113.1(2)	3.1(2)	108.9(13)
$NbH_{0.920}$: $I_I = 0.857(15)$, $I_{II} = 0.143(15)$ or $I_I = 1.0$					
T (K)	E_z^I (meV)	σ_z^I (meV)	E_z^{II} (meV)	σ_z^{II} (meV)	
13	121.6(2)	2.4(1)	112.8(3)	0.7(2)	
77	121.5(1)	2.5(1)	112.5(1)	1.1(1)	
133	121.0(1)	2.7(1)	112.5(2)	2.3(2)	
150	120.8(1)	2.6(1)	112.9(4)	3.3(3)	
190	120.0(1)	3.1(1)			
250	119.5(1)	3.2(1)			
$NbH_{0.945}$: $I_I = 1.0$					
T (K)	E_z^I (meV)	σ_z^I (meV)			
77	121.4(1)	2.7(1)			
133	121.1(1)	2.8(1)			
190	120.8(1)	2.7(1)			

This is also true for the sample $NbH_{0.920}$. In addition to triplet I, which is very similar to that measured for the β phase, a second triplet (II) is visible with peaks at 113, 146 and 157 meV in

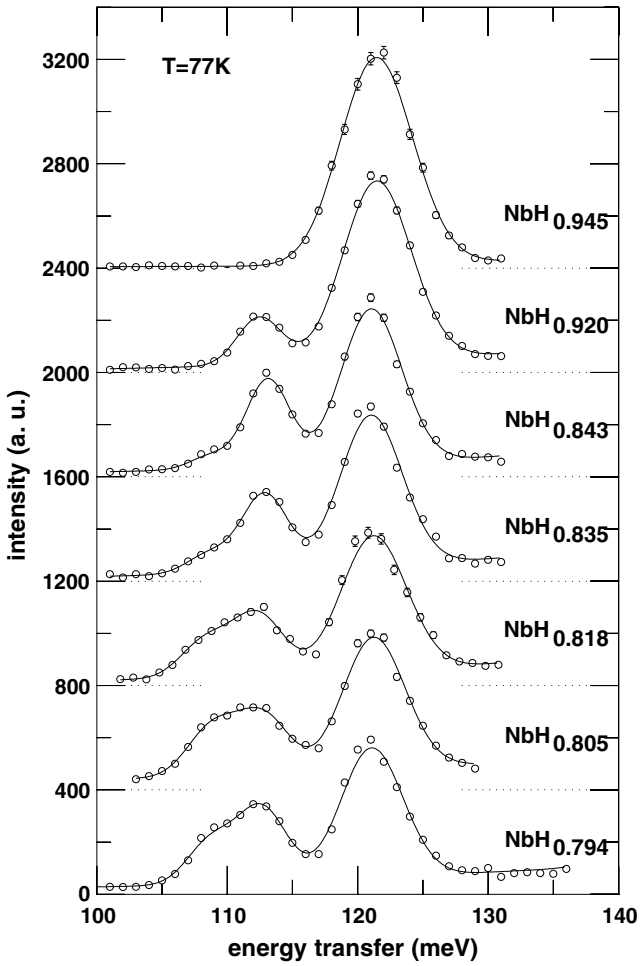

Figure 5. The bgf spectra measured for samples NbH_x with $x > 0.73$ at $T = 77$ K.

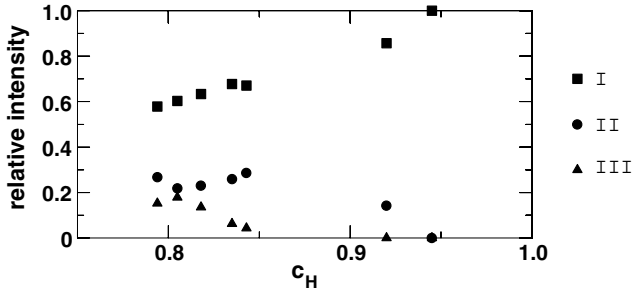

Figure 6. Relative intensities of the peaks I, II and III in the bgf spectra depending on the hydrogen content of the samples at low temperatures ($T = 77$ K).

this case (table 5). The latter is only observed as a shoulder of the peak $\hbar\omega^{\mathrm{I}}_{x,y}$. All bf spectra measured at 13 K are collected in figure 8.

The bgf spectra of the deuterides. The bgf spectra of the deuteride samples $NbD_{0.788}$, $NbD_{0.852}$ and $NbD_{0.922}$ have been measured at 13 K between 70 and 140 meV in order to investigate the isotope effect and to collect vibration and diffraction data on the same samples. The spectrum

Table 2. The bf spectra of the fundamental vibrations measured for $NbH_{0.794}$, fitted with two peak triplets.

$NbH_{0.794}$ intensities: $I_I = 0.582$, $I_{II} = 0.418$ or $I_I = 1.0$				
T (K)	E_z^I (meV) $E_{x,y}^I$ (meV)	σ_z^I (meV) $\sigma_{x,y}^I$ (meV)	E_z^{II} (meV) E_y^{II} (meV) E_x^{II} (meV)	σ_z^{II} (meV) σ_y^{II} (meV) σ_x^{II} (meV)
13	120.9(1) 171.5(2)	2.0(2) 3.8(2)	110.9(2) 145.7(3) 160.2(3)	2.6(2) 4.4(4) 2.4(3)
77	121.2(2) 171.6(1)	1.9(2) 3.9(2)	110.9(2) 146.0(3) 160.5(2)	2.9(3) 6.0(3) 2.6(2)
133	120.8(2) 171.4(1)	2.3(2) 3.8(2)	111.5(2) 148.5(5) 160.8(2)	4.0(3) 7.2(4) 3.5(3)
190	120.2(2) 170.7(3)	3.2(3) 4.6(3)	111.3(5) 146.4(2) 158.9(5)	4.7(5) 8.0(14) 4.8(5)
250	117.7(2) 163.6(3)	3.8(3) 7.4(3)		

Table 3. The bf spectra of the fundamental vibrations measured for $NbH_{0.818}$, fitted with two peak triplets.

$NbH_{0.818}$ intensities: $I_I = 0.603$, $I_{II} = 0.397$				
T (K)	E_z^I (meV) $E_{x,y}^I$ (meV)	σ_z^I (meV) $\sigma_{x,y}^I$ (meV)	E_z^{II} (meV) E_y^{II} (meV) E_x^{II} (meV)	σ_I^{II} (meV) σ_y^{II} (meV) σ_x^{II} (meV)
13	121.5(2) 171.2(2)	2.2(2) 4.3(2)	110.7(3) 144.3(4) 158.1(3)	2.9(2) 6.1(3) 1.3(4)
77	121.2(2) 171.1(2)	2.1(2) 4.3(2)	111.0(3) 144.5(5) 158.3(3)	3.3(2) 7.0(4) 1.8(3)
133	120.6(2) 170.7(3)	2.6(2) 4.2(2)	111.0(4) 144.9(7) 158.2(5)	4.2(2) 8.1(6) 3.2(4)
190	120.3(2) 170.1(3)	2.5(2) 4.3(2)	111.6(3) 148.5(8) 158.7(5)	4.3(3) 7.3(6) 2.8(4)

of $NbD_{0.852}$ (figure 9) exhibits two peak triplets, which are very similar to those measured for $NbH_{0.843}$. The triplet II is probably not a superposition of two triplets since the peak widths are very small (table 6). Also for $NbD_{0.788}$ there seem to be only two triplets. However, the peaks of the triplet II are all broadened, probably due to two unresolved peaks as observed in the hydrides.

The spectrum of $NbD_{0.922}$ exhibits a surprising result (figure 10). In addition to peak I, two peaks were observed below 100 meV: one peak at 79 meV and another one at 74 meV

Table 4. The bf spectra of the fundamental vibrations measured for $NbH_{0.843}$, fitted with two peak triplets.

$NbH_{0.843}$ intensities: $I_I = 0.638$, $I_{II} = 0.362$				
T (K)	E_z^I (meV) $E_{x,y}^I$ (meV)	σ_z^I (meV) $\sigma_{x,y}^I$ (meV)	E_z^{II} (meV) E_y^{II} (meV) E_x^{II} (meV)	σ_z^{II} (meV) σ_y^{II} (meV) σ_x^{II} (meV)
13	121.0(2) 170.1(2)	1.4(2) 3.7(2)	113.0(2) 148.4(4) 159.0(2)	1.4(2) 4.9(3) 0.1(5)
77	120.8(2) 170.0(2)	1.5(2) 3.6(2)	112.9(2) 148.3(4) 159.0(4)	1.9(2) 4.4(4) 0.1(5)
133	120.6(2) 169.8(2)	1.6(2) 3.5(2)	113.1(3) 149.6(5) 159.3(4)	2.9(2) 5.2(4) 1.6(4)
190	119.9(2) 168.8(3)	2.6(2) 4.0(2)	112.9(3) 149.3(4) 158.6(3)	4.0(3) 5.1(4) 1.6(5)

Table 5. The bf spectra of the fundamental vibrations measured for $NbH_{0.920}$, fitted with two peak triplets.

$NbH_{0.920}$ intensities: $I_I = 0.817$, $I_{II} = 0.183$ or $I_I = 1.0$				
T (K)	E_z^I (meV) $E_{x,y}^I$ (meV)	σ_z^I (meV) $\sigma_{x,y}^I$ (meV)	E_z^{II} (meV) E_y^{II} (meV) E_x^{II} (meV)	σ_z^{II} (meV) σ_y^{II} (meV) σ_x^{II} (meV)
13	121.4(2) 166.5(3)	1.9(2) 4.7(2)	112.7(6) 145.9(3) 157.3(5)	0.1(5) 5.4(8) 0.9(8)
77	121.4(2) 166.5(3)	1.9(2) 4.7(2)	112.7(6) 146.2(6) 157.2(5)	0.1(5) 4.8(7) 0.8(8)
250	119.3(2) 162.5(3)	2.7(2) 7.0(3)		

(table 6). The peak positions are at much lower energy transfers than those obtained for other deuterides. The intensity ratio of the additional peaks is 2.1(5). It is difficult to determine the energy of the other fundamental vibrations since the peaks corresponding to the vibrations in the x and y directions could not be resolved. Therefore the fit parameters may only be taken as estimates.

4.2. Neutron diffraction data

4.2.1. Data analysis. One part of the analysis of the neutron diffraction patterns was performed by means of the Rietveld profile refinement method [15] using the program DBW3.2 [16] as already described in [4]. The reliability of the fit is described by the Bragg R value R_B:

$$R_B = \frac{\sum_{hkl} |I_{hkl} - I_{hkl}^c|}{\sum_{hkl} I_{hkl}} \tag{8}$$

Table 6. The bgf spectra of the fundamental vibrations measured for niobium deuterides at $T = 13$ K, fitted with two peak triplets. The two values of E_z^{II} for the sample $NbD_{0.922}$ describe the splitting of this peak.

Sample	Peak system I		Peak system II	
	E_z (meV) $E_{x,y}$ (meV)	σ_z (meV) $\sigma_{x,y}$ (meV)	E_z (meV) E_y (meV) E_x (meV)	σ_z (meV) σ_y (meV) σ_x (meV)
$NbD_{0.788}$	90.4(2)	1.0(2)	84.8(2)	1.4(2)
$T = 13$ K	125.8(3)	2.4(3)	111.4(3)	2.0(3)
			120.8(5)	2.7(5)
$NbD_{0.852}$	90.4(2)	1.1(1)	85.7(3)	0.1(1)
$T = 13$ K	125.1(3)	2.8(2)	112.4(3)	1.7(3)
			118.7(4)	1.0(4)
$NbD_{0.922}$	90.4(2)	1.8(1)	73.6(4)	1.8(2)
$T = 13$ K			79.2(3)	
	122.8(3)	3.2(2)	116.3(15)	6.8(23)
			118.2(7)	2.1(7)

Table 7. Parameters of the Rietveld analysis assuming the structure of the β phase.

Sample	$NbD_{0.715}$		$NbD_{0.788}$
temperature (K)	220	250	250
a (Å)	4.8084(1)	4.8102(1)	4.8169(1)
b (Å)	4.8597(1)	4.8601(1)	4.8709(1)
c (Å)	3.4248(1)	3.4252(1)	3.4372(1)
$\beta_{xx}^D = \beta_{yy}^D$	0.0049(4)	0.0051(4)	0.0108(4)
β_{zz}^D	0.038(2)	0.039(2)	0.033(2)
B_{Nb} (Å^2)	0.32(2)	0.36(2)	0.12(2)
	$NbD_{0.852}$	$NbD_{0.922}$	
	250	173	250
a (Å)	4.8246(1)	4.8277(1)	4.8296(1)
b (Å)	4.8816(1)	4.8948(1)	4.8963(1)
c (Å)	3.4493(1)	3.4625(1)	3.4636(1)
$\beta_{xx}^D = \beta_{yy}^D$	0.0074(4)	0.0075(4)	0.0106(4)
β_{zz}^D	0.035(2)	0.035(2)	0.034(2)
B_{Nb} (Å^2)	0.22(2)	0.22(2)	0.31(2)

where I_{hkl} is the integrated intensity of the Bragg peak hkl and I_{hkl}^c is the calculated intensity. I_{hkl} and I_{hkl}^c do not contain background contributions [17]. The Rietveld program was used to refine the β phase diagrams. The program was also used to refine lattice parameters for the λ phases using the β phase structure model. Since the Rietveld program was not capable of calculating incommensurately modulated superstructures, a different approach was used to analyse the satellite reflections. Peak positions and integrated peak intensities of individual reflections in the λ phase diagrams were determined. Peak positions were used to determine and refine the modulation vectors $\vec{k}$. Integrated intensities were used to refine model parameters using the least squares program POWLS [18] which also allows the analysis of commensurate and incommensurate superstructures [19]. The program allowed the comparison of calculated

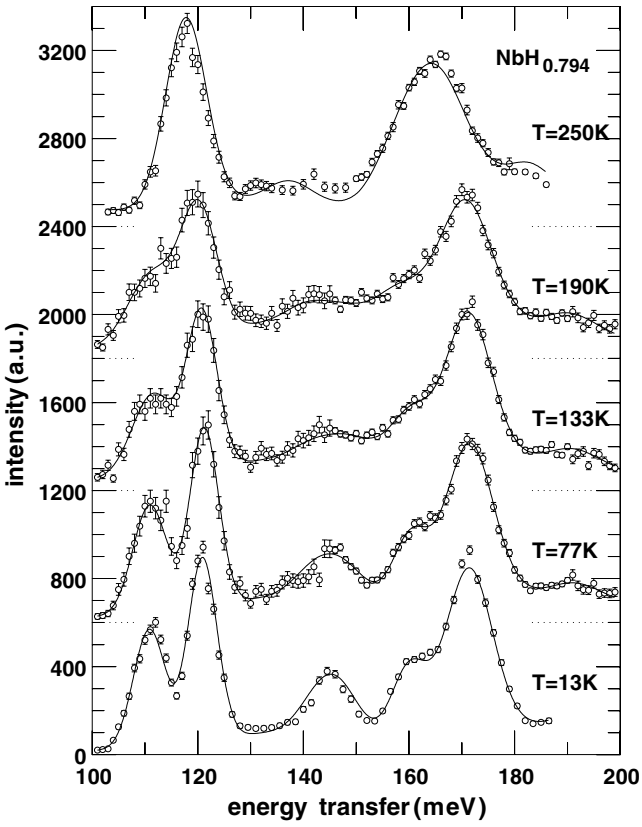

Figure 7. The bf spectra measured for $NbH_{0.794}$.

and measured intensities. However, the refinement of very complex modulated nonmagnetic structures was not possible and had therefore to be done by a 'trial and error' procedure. Within this paper, diffraction patterns can only be presented partly. All diffraction patterns are presented in [14].

4.2.2. Diagrams measured at 250 K: the β phase. Diffraction data have been obtained at 250 K for all deuteride samples including $NbD_{0.715}$, which has already been presented in [4], and $NbH_{0.794}$. Taking into account isotropic temperature coefficients and a small α phase contribution in the case of $NbD_{0.715}$, the structure model of the β phase [20] was confirmed for all samples. The R_B values are between 7% and 9% for most of the samples. For $NbD_{0.922}$, R_B is only 13% indicating an incomplete description of the structure. The quality of the fit could not be improved by allowing other tetrahedral sites to be occupied.

The lattice constants of the deuterides (table 7) depend nearly linearly on the deuterium concentration c_D:

$$a_0(c_D) = 4.741\ \text{Å} + c_D \cdot 0.097\ \text{Å}, \tag{9}$$

$$b_0(c_D) = 4.734\ \text{Å} + c_D \cdot 0.174\ \text{Å}, \tag{10}$$

$$c_0(c_D) = 3.291\ \text{Å} + c_D \cdot 0.187\ \text{Å}. \tag{11}$$

The lattice parameters of the sample $NbH_{0.794}$ are more than 0.01 Å larger than those of $NbD_{0.788}$.

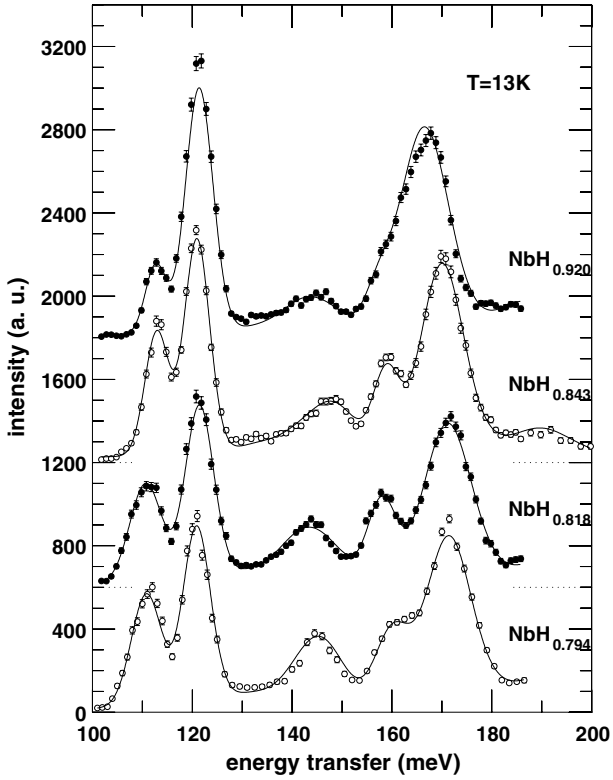

Figure 8. The bf spectra measured for samples NbH_x with $x > 0.73$ at $T = 13$ K; fitted using two peak triplets.

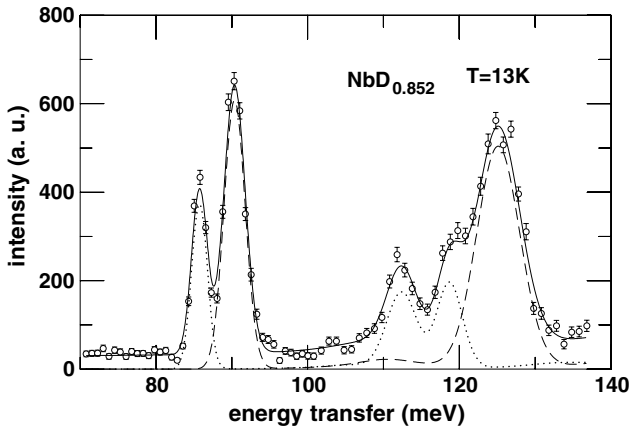

Figure 9. The bgf spectrum measured for $NbD_{0.852}$ at $T = 13$ K.

4.2.3. Diagrams measured below 200 K: λ phases. First of all a reliable structure model was deduced from the diffraction patterns of $NbD_{0.788}$. A Rietveld analysis has been performed using the β phase structure model since the peaks dominated by the scattering contribution of the niobium atoms allow one to determine the lattice constants (table 8). Many peaks affected by a hydrogen contribution are split into satellite peaks, which is in accordance with observations by Brun *et al* [7].

We examined the structure model proposed in [5, 7] using the program POWLS in a first trial. We chose $k_z = 0.2$ corresponding to a deuterium concentration of $c_D = 0.8$ due to

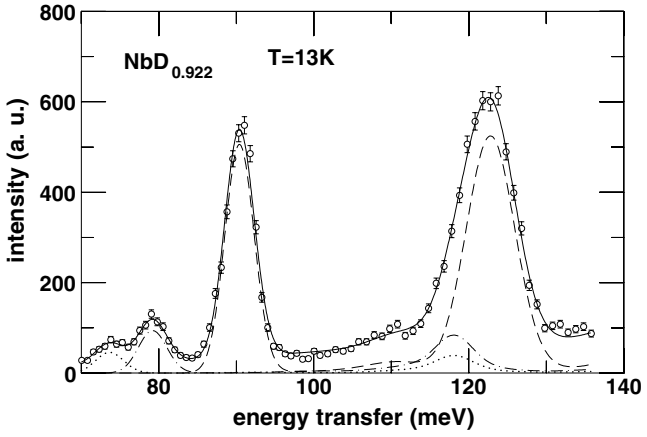

Figure 10. The bgf spectrum measured for $NbD_{0.920}$ at $T = 13$ K.

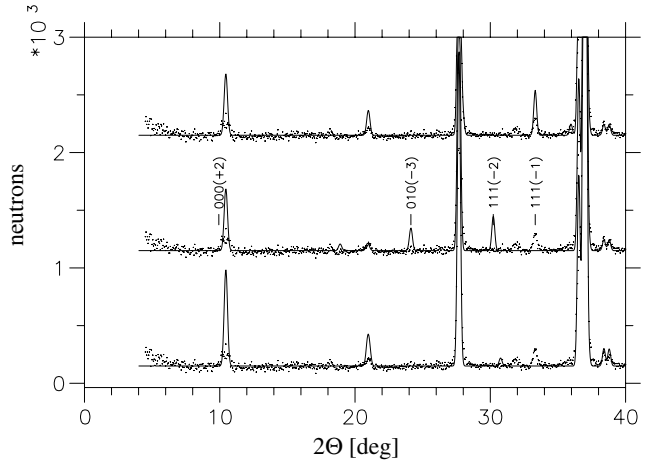

Figure 11. The diffraction pattern of $NbD_{0.788}$ at $T = 13$ K. A POWLS calculation assuming $k_z = 0.2$ and a zigzag ordering of intrinsic vacancies within the microdomain boundaries.

Table 8. Lattice constants of the sample $NbD_{0.788}$ (Rietveld analysis of the Bragg peaks dominated by the niobium contribution).

Temperature (K)	Lattice constants		
	a (Å)	b (Å)	c (Å)
13	4.817	4.868	3.430
77	4.817	4.868	3.431
133	4.816	4.869	3.432
190	4.815	4.871	3.433
250	4.814	4.868	3.435

the existence of intrinsic deuterium vacancies within the microdomain boundaries. A zigzag ordering of the intrinsic vacancies was assumed as suggested in [5, 7]. A good description of both the positions and the intensities of the satellite peaks was achieved (figure 11). The reliability of the fit is $R_B = 12\%$. Therefore this model is correct in principle.

In the following we treat the questions concerning the exact value of k_z, the structure of the microdomain boundaries, the displacements of the atoms within these boundaries and the regularity of the distances between the boundaries.

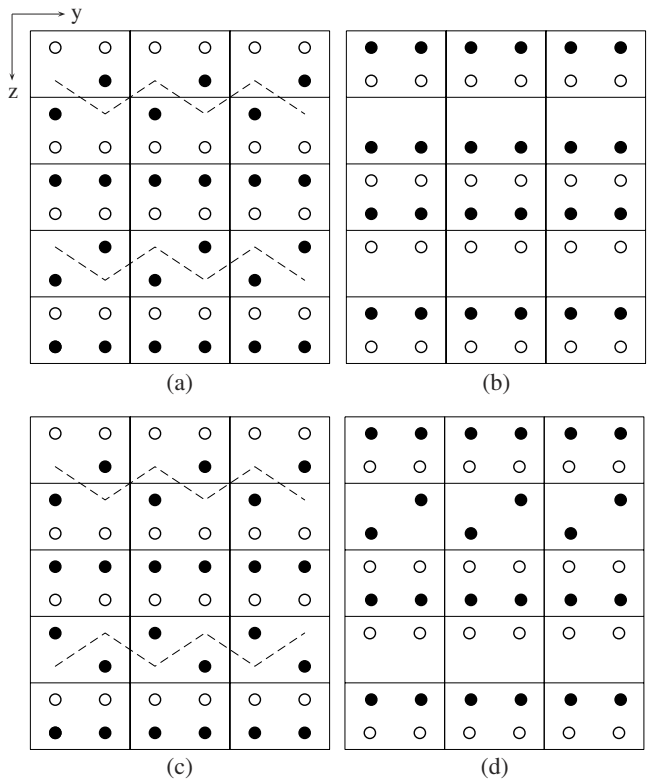

Figure 12. The structure model of the λ phases according to [7] using different structure models of the microdomain boundaries: (a) top left: zigzag model A; (b) top right: plain layer model; (c) bottom left: zigzag model B; (d) bottom right: 'mixed' model. •, $x = \frac{1}{4}$; ∘, $x = \frac{3}{4}$. The niobium atoms are not shown.

The component k_z was determined by a least squares fit to be $k_z = 0.203(3)$. The error includes the statistical error as well as the uncertainty concerning the lattice constants and the zero point determined by the Rietveld method.

We performed calculations introducing different models of the microdomain boundaries: two kinds of zigzag models, denoted by A and B, and a model using plain layers of vacancies (see figure 12). We chose $k_z = 0.203$ in each case and did not introduce any displacements of the atoms from their ideal position in a β phase cell.

The observed diffraction patterns are best described by the zigzag model A as shown in figure 13, partly. The peaks 111(−1), 111(+1), 131(−1) and 131(+1), e.g., can only be explained by the zigzag model A. Furthermore, the peaks 010(−3) and 111(−2) are not visible, in contradiction to calculations according to zigzag model B.

Atom positions and isotropic temperature coefficients of the zigzag model A and the plain layer model have been varied in order to improve the agreement between calculated and observed intensities. We varied the parameters which describe the positions of the atoms in the vicinity of the microdomain boundaries as indicated in figure 14. These parameters should exhibit the largest deviations from their ideal values in the β phase cell. All displacements show the expected direction as indicated in figure 14. The magnitudes of the displacements are similar to those obtained in the case of the ε phase (table 9). The R_B value was improved for both models ($R_B = 7.5\%$).

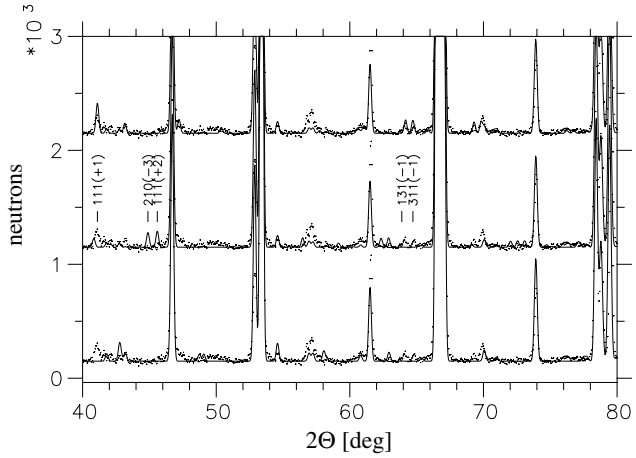

Figure 13. The diffraction pattern of $NbD_{0.788}$ at $T = 13$ K. A POWLS calculation for the region $0° < \text{deg} < 40°$ (left) and $40° < \text{deg} < 80°$ (right) assuming three different models for the microdomain boundaries: top: zigzag model A; centre: zigzag model B; bottom: plain layer model.

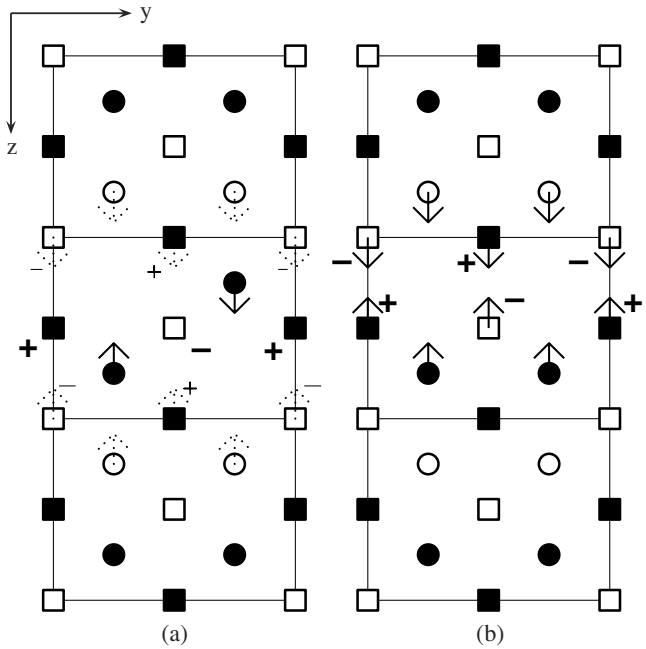

Figure 14. Displacements of the atomic positions introduced for the zigzag model (left) and the plain layer model (right) shown in the projection of the structure onto the y–z plane. The symbols describe the x value of the atomic position: niobium atoms: □, $x = 0$; ■, $x = 0.5$; hydrogen atoms: ○, $x = 0.25$; ●, $x = 0.75$. The arrows indicate the direction of the displacements within the y–z plane; the (+, −) signs indicate the displacements in the direction of the x axis.

Nevertheless, for the plain layer model the main differences between the calculated and observed diffraction patterns remain, since not all peaks can be described by this model. Therefore we reject this model for the exclusive explanation of this particular diagram.

Table 9. Atomic displacements compared with the β phase structure in the fits of the diffractograms of the sample $NbD_{0.788}$ measured at 13 K, for the plain layer model and the zigzag model A.

	Plain layer model			Zigzag model A				
	Neighbouring layer			Zigzag layer		Neighbouring layer		
	z_D	x_{Nb}	z_{Nb}	z_D	x_{Nb}	z_D	x_{Nb}	z_{Nb}
$\Delta(x, z)$ (Å)	0.09	0.07	0.02	0.13	0.10	0.04	0.02	0.01
Δr (Å)	0.09	0.07		0.13	0.10	0.04	0.03	

Table 10. Lattice constants of the sample $NbH_{0.794}$ obtained by analysing the Bragg peaks dominated by the scattering contributions of the niobium lattice.

Temperature (K)	Lattice constants		
	a (Å)	b (Å)	c (Å)
13	4.818	4.884	3.432
133	4.816	4.886	3.433
190	4.818	4.887	3.434
250	4.828	4.884	3.437

However, taking into account alternating zigzag layers and plain layers as microdomain boundaries, those peaks can also be described. Therefore we cannot decide whether there is an additional contribution of plain layers to the zigzag model A.

The diffraction data collected at 77 and 13 K do not show any significant differences. Those peaks which are not described by the plain layer model become weaker at 133 K and vanish at 190 K. All other peaks do not vanish. This indicates a change from the zigzag layer model to a plain layer model of the microdomain boundaries. The lattice constants (table 8) show an anomalous behaviour at 133 and 190 K since the lattice parameter a_0 decreases with increasing temperature.

Diffraction patterns were measured for the sample $NbH_{0.794}$ at 13, 133 and 190 K. The analysis using POWLS confirmed that these data can also be described by a structure model consisting of sequences of differently oriented β phase cells. The data did not allow us to distinguish between different structure models of the microdomain boundaries. The analysis yielded $k_z = 0.0196(5)$. The lattice constants obtained by the Rietveld analysis are given in table 10.

The analyses of the $NbD_{0.852}$ diffraction patterns show a general agreement between calculated and measured count rates in the case of the plain layer model as well as in the case of the zigzag layer model. However, both models propose a group of satellite peaks that are missing in the measured diagrams, and both models fail to explain three observed small peaks in the diffraction patterns. Furthermore, pairs of peaks with permuted indices h and k associated with a tetragonal unit cell could not be resolved any longer, as they were in the case of $NbD_{0.788}$. Nevertheless, an appropriate structure model for $NbD_{0.852}$ could not be found. The model of the γ phase proposed by Hauck [11] failed to describe the data. The value of k_z was determined to be 0.147(5) using the model proposed by Brun *et al* [7]. A tetragonal symmetry was assumed in order to obtain the lattice constants by the Rietveld method (table 11).

At all temperatures the diagrams of the sample $NbD_{0.922}$ are dominated by a β phase contribution. At 133 K and lower temperatures additional peaks are observed. These peaks can be attributed to a second phase and indicate a tetragonal or cubic symmetry of the structure. In addition, eleven very weak satellite peaks are observed as for $NbD_{0.852}$. We calculated $k_z = 0.168(5)$.

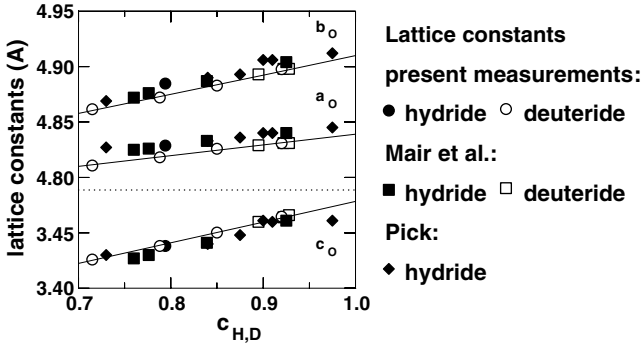

Figure 15. Lattice constants a_0, b_0 and c_0 compared to the values from [9, 24] and [25]. The linear fit of the concentration dependence of the lattice constants according to the measurements is shown.

Table 11. Lattice constants of the sample $NbD_{0.852}$ obtained by analysing the Bragg peaks dominated by the scattering contributions of the niobium. A tetragonal unit cell was assumed for temperatures below 200 K.

Temperature (K)	Lattice constants		
	a (Å)	b (Å)	c (Å)
13	4.852		3.441
77	4.852		3.442
133	4.853		3.442
190	4.854		3.443
250	4.825	4.882	3.449

Table 12. Fundamental hydrogen vibrations investigated in earlier measurements of the β phase at $T = 300$ K.

Sample	$\hbar\omega_z$ (meV)	$\hbar\omega_{x,y}$ (meV)	Reference
$NbH_{0.32}$	116.0(7)	167.0(15)	[22]
$NbH_{0.82}$	119.0(2)	166.8(5)	[21]
$NbH_{0.87}$	119(1)	164(1.5)	[12]
$NbH_{0.92}$	118(1)	162(2)	[12]
$NbH_{0.95}$	118(1)	163(2)	[12]
$NbD_{0.72}$	86(1)	120(1.5)	[22]
$NbD_{0.85}$	87.2(2)	118.1(3)	[21]

5. Discussion

5.1. The β phase

The vibrational spectra and the diffraction patterns show a good agreement with the well established model of the β phase structure and the vibrations of the hydrogen atoms therein. The single peak triplet is attributed to the single kind of hydrogen site within the structure. The vibrational data also agree well with the data measured earlier (table 12) [12, 21, 22]. However, the problems concerning the shape of the peaks in the vibrational spectrum of $NbH_{0.920}$ and the peak intensities in the $NbD_{0.922}$ diagrams cannot be solved yet. It is interesting to note that Kuji and Oates [23] detected changes of the thermodynamics at hydrogen concentrations $c_H > 0.9$. All these results may be caused by a disturbance of the ideal lattice of the β phase.

The lattice parameters derived from the neutron diffraction data complete the data collected by Pick [9, 24] and Mair [25] (see figure 15). The temperature dependence of the lattice

parameters is in agreement with earlier investigations. The results agree very well with regard both to the hydrides and to the deuterides and confirm the isotopic dependence of the lattice constants even for hydrogen concentrations $0.7 < c_{H,D} < 0.9$. The lattice parameters a_0 and b_0 are 0.01 Å larger for hydrides than for deuterides.

5.2. λ phases

5.2.1. Vibrational spectra. Three peak systems are visible in all vibrational spectra measured for samples with hydrogen concentrations in the region $0.79 < c_H < 0.85$ below 190 K. These spectra can be attributed to the λ phase region. The phase boundary between the λ phase regime and the β phase is located at a temperature between 190 and 250 K for $NbH_{0.794}$. A further phase transition could not be clearly identified in this region, but a transition around 100 K cannot be excluded since the broadening of the line triplets II and III may cover a shift of intensities or the disappearance of one of these peak systems.
The phase transition from the β phase to the λ phase region was established between 150 and 190 K for $NbH_{0.920}$. $NbH_{0.945}$ stays in the β phase regime down to 77 K.
The position of peak I decreases with increasing temperature for all samples which may be connected with the thermal expansion of the niobium lattice.
A phase transition can be deduced from the disappearance of the peak system III around $c_H = 0.85$ at least below 77 K as well as of the peak system II around $c_H = 0.93$ between 77 and 190 K. In addition, a two-phase region must exist between $c_H = 0.715$ [4] and $c_H = 0.794$. Nevertheless, the sample $NbH_{0.794}$ does not belong to this two-phase region since the characteristic peaks of the ε phase are missing.
Taking into account this information on the phase diagram and the dependence of the peak intensities on the hydrogen concentration, one can show that at least two phases exist in the region between the ε phase and the phase at $c_H = 0.85$. Furthermore, at least one of these phases must exhibit three different hydrogen sites. Nevertheless, the data are much easier to interpret if the existence of incommensurate phases for $c_H < 0.85$ is assumed.
The vibrational spectra of the deuterides with $c_D < 0.9$ measured at 13 K are in accordance with those of the hydrides. However, a remarkable isotopic effect exists for hydrogen concentrations $c_H > 0.9$ since neither the number of the peak systems nor the position of the additional peaks for $NbD_{0.922}$ corresponds to those found for the hydride samples.

5.2.2. Structure investigations. We assume the same structures for hydrides and deuterides for hydrogen concentrations $c_H < 0.85$ since the vibrational spectra as well as the diffraction data do not show any significant differences between hydrides and deuterides. The three peak systems can be related to three hydrogen sites with different hydrogen surroundings analogous to the ε phase [4]. The peak triplet I is attributed to hydrogen sites in the model proposed by Brun *et al* [7], having the same local environment as the ideal site of the β phase. This assignment is independent of the special models of the microdomain boundaries mentioned above.

The hydrogen sites within the microdomain boundaries are surrounded by distorted niobium tetrahedra. Therefore the peak triplets II and III which indicate a strong deviation from the ideal tetrahedral site symmetry may be attributed to these sites. Assuming a non-Gaussian distribution of potentials, both triplets II and III can be combined and attributed to the sites in one special microdomain boundary (plain or zigzag layer boundary). On the other hand, assuming the coexistence of the two kinds of microdomain boundaries, one triplet may be attributed to the hydrogen sites within the plain layer boundaries and the other to the sites within the zigzag layer boundaries. The latter case seems to be more probable since it is the easiest way to explain the existence of two peak systems in addition to triplet I.

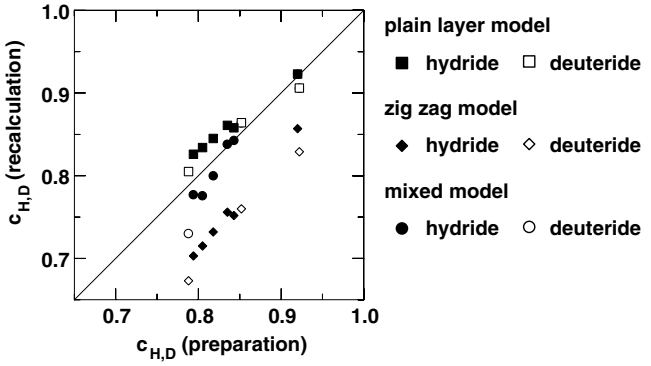

Figure 16. Recalculated hydrogen concentrations $c_{H,D}$ obtained using the intensity ratios of the three peak triplets that could be resolved in the bgf spectra, depending on the hydrogen concentration determined by the weight increase of the samples. The recalculated values should hit the solid line in the best case. For $c_{H,D} > 0.85$ a difference between the plain layer model and the 'mixed' model does not exist since only two peak systems could be resolved.

In any case, the intensity ratio of the three triplets allows a recalculation of the total hydrogen concentration (figure 16) since each hydrogen site is associated with a typical number of additional intrinsic vacancies. The recalculated values are far too low in the case of the pure zigzag layer model which is therefore rejected. Since the plain layer model is not in accordance with the diffraction pattern of $NbD_{0.788}$ below 100 K, this model can also be rejected, although it would harmonize roughly with the recalculations of the hydrogen concentration described above. Therefore, only the 'mixed' model taking into account both kinds of domain boundaries can explain both the diffraction patterns and the intensity ratios of the peak systems in the vibrational spectra. The deviation of the recalculated and the measured hydrogen concentration in the case of $NbD_{0.788}$ may be due to the incomplete separation of triplet II and III which prevents a proper determination of their intensity ratio. The disappearance of characteristic satellite peaks in the diffraction patterns of $NbD_{0.788}$ above 100 K indicates a transition to a phase with pure plain layer microdomain boundaries. In agreement with the vibrational spectra of $NbH_{0.794}$, the transition to the β phase takes place between 190 and 250 K.

A phase transition is clearly recognized at $c_{H,D} = 0.85$ which seems to be connected with the disappearance of zigzag layer microdomain boundaries. Furthermore, the data indicate the existence of a highly symmetric modulated structure in this concentration regime. A remarkable difference exists between hydrides and deuterides concerning the number of hydrogen sites with distorted tetrahedral symmetry for hydrogen concentrations $c_H > 0.9$. The transition to the β phase is visible in the diffraction patterns as well as in the inelastic data.

5.2.3. Comparison with the results of previous investigations. The basic model for hydrogen concentrations $0.78 < c_{H,D} < 0.85$ has been suggested previously by Brun *et al* [7]. It is based on experiments on niobium deuterides within $0.72 < c_D < 0.85$. In that work the group could neither decide between the different possible structures of the microdomain boundaries nor make any statements concerning the displacements of the hydrogen atoms. Similar to our results, the k_z values determined by Brun *et al* are slightly smaller than $(1 - c_D)$. Brun *et al* assume the boundaries of this special phase region to be at $c_H = 0.78$ and 0.85. This is in very good agreement with our results and the diffraction measurements on $NbD_{0.825}$ of Welter and Schöndube [10].

Pick [9] proved the existence of a highly symmetric (cubic) γ phase by means of x-ray measurements on samples with $c_H \approx 0.9$, in good agreement with our results. Small differences concerning the exact position of the phase transitions around $c_{H,D} = 0.85$ and 0.92 may be explained by isotope effects.

Makenas and Birnbaum [5, 8] investigated niobium hydrides at hydrogen concentrations $0.85 \leqslant c_H \leqslant 1.07$ by means of electron microscopy. Taking into consideration an isotope effect they found the same phases as Brun *et al* [7] at lower hydrogen concentrations. Our results show that at very high hydrogen concentrations $c_{H,D} > 0.9$ similar values of k_z to those determined at hydrogen concentrations $c_H < 0.85$ exist, but related with higher symmetry structures. Furthermore, the assumption of Makenas and Birnbaum that only three phases with k_z values of 3/14, 3/16 and 3/18 exist within the total concentration range has not been confirmed by our results (with $k_z \approx 3/15$).

Concerning the phase boundaries, our results can be compared with the phase diagram proposed by Köbler and Welter [6] who determined the phase ι at $c_H = 0.78$ as the phase with the lowest hydrogen concentration in the λ phase region. This result is in agreement with our investigations as well as with Brun *et al* [7] and Makenas and Birnbaum [5, 8]. Our data show that a region of incommensurately modulated phases is probably located at higher hydrogen concentrations $0.78 < c_H < 0.85$. This is in agreement with Brun *et al* [7] who observed only pure phases at concentrations $c_H < 0.85$ but not a two-phase region, confirmed by theoretical contributions of Kajitani *et al* [26] and Vaks *et al* [27]. The phase transition observed by Köbler and Welter [6] at $c_H = 0.83$, however, is not confirmed by the data nor is the transition at $T \approx 70$ K. The transition above 100 K is confirmed by our diffraction measurements. This phase transition may be correlated with the one detected in [28] around 100 K at concentrations $0.82 < c_H < 0.93$.

In the region $c_{H,D} < 0.85$ no significant deviations between hydrides and deuterides as regards the phase diagram could be detected. This is only partially true for higher hydrogen concentrations $c_{H,D} > 0.85$ as already mentioned above. The structure of these phases is not yet known. But the phase with the highest hydrogen concentration can be established at $c_{H,D} = 0.9$ in accordance with Köbler and Welter [6] and Pick [9]. However, a deviation between the phase diagrams of Nb–H and Nb–D in this region is indicated by the vibrational spectra and seems to be quite possible.

Summarizing the results, the following clear deviations have been found in relation to the phase diagram proposed by Köbler and Welter [6]. The existence of the ν phase at $x = 0.83$ cannot be confirmed. Furthermore, the phase transition at $T \approx 70$ K between $x = 0.78$ and 0.85 cannot be confirmed either. In addition, the region of the pure β phase can be extended approximately to $x = 0.94$ even at low temperatures around $T = 77$ K. Nevertheless, a phase transition around $T = 100$ K between $x = 0.78$ and 0.85 cannot be excluded. At these concentrations a region of incommensurately modulated phases seems to be most probable, possibly with different microdomain structures above 100 K and below 100 K. The phases ι, ξ and γ proposed by Köbler and Welter [6] are in accordance with our results. The results are visualized in a simplified phase diagram (figure 17). However, since we cannot make any statements on the phases o, λ and μ we did not take them into account, although they may exist. In addition, the introduced phase transitions have to be regarded as a rough indication of their position only.

Earlier vibrational spectra [12, 21] agree well with our measurements (see table 13). Larger discrepancies exist for $NbH_{0.794}$ and $NbH_{0.78}$ [12]. This may indicate an additional phase at $c_H \approx 0.78$. The $NbH_{0.87}$ spectra show a splitting [12], perhaps due to the existence of different hydrogen sites within one phase.

Table 13. Comparison of the fundamental hydrogen vibrations investigated in earlier measurements [12, 21] with the measurements presented now ('New'). Averaging over new data peaks which could not be resolved in the earlier experiments was performed in order to enable a better comparison.

Sample	T (K)	$\hbar\omega_z$ (meV)		Reference
$NbD_{0.80}$	78	84.8(8)	88.6(8)	[12]
$NbD_{0.788}$	13	84.8	90.4	New
$NbD_{0.85}$	10	88.4(3)		[21]
$NbD_{0.852}$	13	88.9		New
$NbH_{0.78}$	78	118.3(9)	126.1(9)	[12]
$NbH_{0.794}$	77	110.9	121.2	New
$NbH_{0.92}$	78	120(1)		[12]
$NbH_{0.920}$	77	119.0		New
$NbH_{0.87}$	78	114(1)	123(1)	[12]
$NbH_{0.87}$	150	115(1)	123(1)	[12]
$NbH_{0.87}$	193	115(1)	124(1)	[12]
$NbH_{0.95}$	15	121.8(8)		[12]
$NbH_{0.95}$	78	121(1)		[12]
	T (K)	$\hbar\omega_{x,y}$ (meV)		Reference
$NbD_{0.80}$	78	116.9(1.5)	124.4(1.5)	[12]
$NbD_{0.788}$	13	116.2	125.8	New
$NbD_{0.85}$	10	121.6(4)		[21]
$NbD_{0.852}$	13	122.1		New
$NbH_{0.78}$	78	167(2)	177(2)	[12]
$NbH_{0.794}$	77 (146.0)	160.5	171.6	New
$NbH_{0.92}$	78	163(1.5)		[12]
$NbH_{0.920}$	77 (146.2)	164.7		New
$NbH_{0.87}$	78	165(1.5)	174(1.5)	[12]
$NbH_{0.87}$	150	163(2)	173(2)	[12]
$NbH_{0.87}$	193	163(2)	172(2)	[12]
$NbH_{0.95}$	15	165.6(1.5)		[12]
$NbH_{0.95}$	78	165(1.5)		[12]

6. Conclusion

We performed neutron vibrational and neutron diffraction measurements on niobium hydrides NbH_x and niobium deuterides NbD_x in the concentration range $0.73 < x < 1.0$ at temperatures $13\ \mathrm{K} \leqslant T \leqslant 250\ \mathrm{K}$. The samples can be assigned to the β phase at 250 K. Taking into account the investigations on samples with lower hydrogen concentrations [4] the neutron diffraction data confirm the structure model proposed by Somenkov *et al* [20]. The neutron vibrational spectra exhibiting a single peak system confirm earlier investigations (see e.g. [21, 22]) and are in agreement with a model of a single type of tetrahedral hydrogen sites in a bcc lattice. Small deviations from this picture for $x > 0.9$, however, are not yet understood. An isotopic effect concerning the lattice parameters found earlier for hydrogen concentrations $x > 0.9$ [25] is confirmed and established even for lower concentrations $0.7 < x < 0.9$.

The vibrational spectra and diffraction patterns measured at temperatures lower than 200 K can be attributed to a region of ordered phases that are summarized as λ phases. The vibrational spectra show up to three peak systems. We attribute these peak triplets to

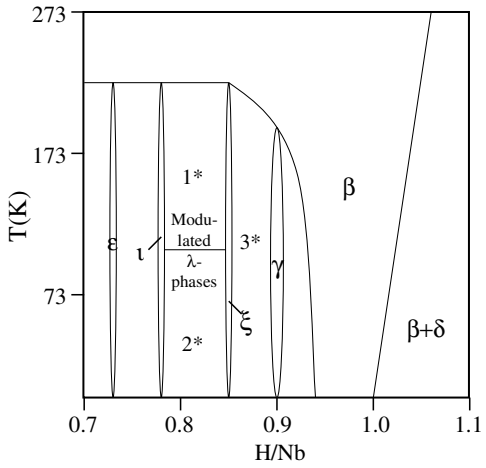

Figure 17. A simplified phase diagram which visualizes the results of the present paper in relation to the results of Köbler and Welter [6]. Between $x = 0.78$ and 0.85 incommensurately modulated phases are probable at low temperatures: region 1*: plain layer model; region 2*: mixed model; region 3*: probably modulated phases with unknown structure.

different hydrogen sites within the structure of the λ phases. We confirmed and refined the structure model proposed by Brun *et al* [7] for $NbD_{0.788}$ and $NbH_{0.794}$ by means of diffraction measurements. Accordingly the structure consists of microdomains with β phase structure. Successive microdomains in the *c* direction are twisted by 180° and build up a modulation of the structure. The wavelength of this modulation is $k_z \approx 1 - c_{H,D}$. The coexistence of two kinds of microdomain boundaries at temperatures below 100 K appears to be very probable if one combines the neutron vibrational spectra and neutron diffraction data: the intrinsic vacancies that form the microdomain boundaries are ordered in plain layers as well as in zigzag layers. One kind of the three different hydrogen sites recognized by means of vibrational spectroscopy can be localized within the microdomains on undistorted tetrahedral sites; the other two can be attributed to two different kinds of microdomain boundaries. The contribution of zigzag layer microdomain boundaries decreases with increasing hydrogen concentration and disappears around $x = 0.85$ and at temperatures higher than 100 K. A region of partly incommensurately modulated phases exists in the concentration range $0.78 < x < 0.85$. However, the existence of a sequence of only commensurately modulated phases cannot be excluded.

At $x \approx 0.85$ a change of symmetry of the unit cell from orthorhombic to a higher symmetry occurs. Furthermore, the modulation changes at even higher hydrogen concentrations $x \geqslant 0.9$. For the λ phase with the largest hydrogen content (γ phase), the numbers of peaks in the vibrational spectra are different for hydrides and deuterides. Our results agree with the results of Pick [9] concerning the higher symmetry of the γ phase and with the investigations of Makenas [5, 8] concerning the modulation vector. The phase diagram proposed in [6] is partly confirmed and can be better understood now. The results allow a better interpretation of earlier investigations using different methods such as muon spin rotation studies [29, 30]. Moreover, the present data will be very useful for verifying theoretical models, e.g. concerning the phase diagram [23] and the hydrogen potential [31–34].

Acknowledgments

The authors would like to thank H J Bierfeld and J M Wilhelm for the preparation of the samples, T Schober for helpful discussions and D Henkel for her valuable support. BH

gratefully acknowledges financial support by the Deutsche Forschungsgemeinschaft in the framework of Graduiertenkolleg 232 in Saarbrücken; RH gratefully acknowledges financial support by the Fonds der Chemischen Industrie.

References

[1] Schober T and Wenzl H 1978 *Hydrogen in Metals II* (*Springer Topics in Applied Physics*) ed G Alefeld and J Völkl (Berlin: Springer)
[2] Wenzl H and Welter J-M 1978 *Current Topics in Materials Science* vol 1, ed E Kaldis (Amsterdam: North-Holland)
[3] Schober T 1995 *Hydrogen Metal Systems I* ed F A Lewis and A Aladjem (Zürich: Seitech)
[4] Hauer B, Hempelmann R, Udovic T J, Rush J J, Jansen E, Kockelmann W, Schäfer W and Richter D 1998 *Phys. Rev.* B **57** 11115
[5] Makenas B J and Birnbaum H K 1982 *Acta Metal.* **30** 469
[6] Köbler U and Welter J-M 1982 *J. Less-Common Met.* **84** 225
[7] Brun T O, Kajitani T, Mueller M H, Westlake D G, Makenas B J and Birnbaum H K 1979 *Proc. Modulated Structures Mtg (Kailua-kona, Hawaii, 1979)*; *AIP Conf. Proc.* **53** 397
[8] Makenas B J 1978 *PhD Thesis* University of Illinois, Urbana
[9] Pick M A 1973 *PhD Thesis* RWTH Aachen
Pick M A 1973 *Berichte der KFA Jülich* Nr. 951-FF, Jülich
[10] Welter J-M and Schöndube F 1983 *J. Phys. F: Met. Phys.* **13** 529
[11] Hauck J 1977 *Acta Crystallogr.* A **33** 208
[12] Eckert J, Goldstone J A, Tonks D and Richter D 1983 *Phys. Rev.* B **27** 1980
[13] Springer T and Richter D 1987 *Methods of Experimental Physics* vol 23B *Neutron Scattering* ed K Sköld and D L Price (London: Academic)
[14] Hauer B 1995 *PhD Thesis* Universität des Saarlandes, Saarbrücken
[15] Rietveld H M 1969 *J. Appl. Crystallogr.* **2** 65
[16] Wiles D B 1982 *Program for Rietveld Analysis of X-Ray and Neutron Powder Diffraction Patterns: DBW3.2* School of Physics, Georgia Institute of Technology, Atlanta, GA 30332
See also: Wiles D B and Young R A 1981 *J. Appl. Crystallogr.* **14** 149
[17] Jansen E, Schäfer W and Will G 1994 *J. Appl. Crystallogr.* **27** 492
[18] Will G 1979 *J. Appl. Crystallogr.* **12** 483
[19] Kockelmann W, Jansen E, Schäfer W and Will G 1995 *Berichte des Forschungszentrums Jülich* Nr. 3024, Jülich
[20] Somenkov V A, Gurskaya A V, Zemlyanov M G, Kost M E, Chernoplekov N A and Chertkov A A 1968 *Sov. Phys.—Solid State* **10** 1076
[21] Richter D and Shapiro S M 1980 *Phys. Rev.* B **22** 599
[22] Rush J J, Magerl A, Rowe J M, Harris J M and Provo J L 1981 *Phys. Rev.* B **24** 4903
[23] Kuji T and Oates W A 1984 *J. Less-Common Met.* **102** 173
[24] Pick M A and Bausch R 1976 *J. Phys. F: Met. Phys.* **6** 1751
[25] Mair G, Bickmann K and Wenzl H 1979 *Z. Phys. Chem. NF* **114** 29
[26] Kajitani T, Brun T O, Mueller M H, Birnbaum H K and Makenas B J 1979 *Proc. Modulated Structures Mtg (Kailua-kona, Hawaii, 1979)*; *AIP Conf. Proc.* **53** 394
[27] Vaks V G, Zein N E, Kamyshenko V V and Tkachenko T V 1988 *Sov. Phys.—Solid State* **30** 270
[28] Melik-Shakhnazarov V A, Byndlinskaya I N, Naskidashvili I A, Arabadzhyan N L and Chachanidze R V 1981 *Sov. Phys.—JETP* **54** 168
[29] Richter D, Hempelmann R, Hartmann O, Karlsson E, Norlin L O, Cox S F J and Kutner R 1983 *J. Chem. Phys.* **79** 4564
[30] Hartmann O, Karlsson E, Wäppling R, Gustavsson-Seidel A, Richter D, Hempelmann R, Kossler W J, Hitti B, Kempton J, Lamkford W F and Stronach C E 1986 *Hyperfine Interact.* **31** 241
[31] Sugimoto H and Fukai Y 1980 *Phys. Rev.* B **22** 670
[32] Sugimoto H and Fukai Y 1981 *J. Phys. Soc. Japan* **50** 3709
[33] Sugimoto H and Fukai Y 1982 *J. Phys. Soc. Japan* **51** 2554
[34] Elsässer C, Ho K M, Chan C T and Fähnle M 1992 *J. Phys.: Condens. Matter* **4** 5207